Int. J. Electrochem. Sci., 13 **(2018)** 7578 – 7589, doi: 10.20964/2018.08.50

International Journal of
ELECTROCHEMICAL
SCIENCE
www.electrochemsci.org

Effects of Citric Acid Treatment on the Electrochemical Properties of $Li_{1.2}Mn_{0.54}Ni_{0.13}Co_{0.13}O_2$ Cathode Material

Bailong Liu[1,2,*], *Zhaohui Zhang*[1,2], *Mei Wu*[1], *Shuxiang Xu*[1]

[1] School of Metallurgical Engineering, Xi'an University of Architecture and Technology, Xi'an 710055, P. R. China
[2] Shaanxi Province Metallurgical Engineering and Technology Research Centre, Xi'an University of Architecture and Technology, Xi'an 710055, P. R. China
[*]E-mail: liubailong@xauat.edu.cn

Received: 6 May 2018 / *Accepted:* 19 June 2018 / *Published:* 5 July 2018

The influence of citric acid pre-activation on the electrochemical properties of cathode materials used in lithium batteries is investigated. During the citric acid pre-activation of the surface of coprecipitated $Li_{1.2}Mn_{0.54}Ni_{0.13}Co_{0.13}O_2$, 13.37 wt.% of lithium is removed, mainly owing to the decomposition of the Li_2MnO_3. Electrochemical property tests indicate that the cycle performance and rate capability of the material are enhanced after citric acid pre-activation. The initial charge-discharge efficiency increases from 66.4% to 79.9%, while the capacity retention after 100 cycles at 0.5C increases from 84.85% to 90.81%. When the current density increases to 5C, the specific discharge capacity of the delithiated material is 108.9 $mAh \cdot g^{-1}$, much higher than that (95.10 $mAh \cdot g^{-1}$) before the treatment. This is caused by the formation of a spinel-like structure on the cathode surface, as citric acid removes some of the Li_2O in the Li_2MnO_3 phase. As a result, a channel for Li^+ transmission is created and the impedance at the interface between the cathode material and the electrolyte is effectively reduced, facilitating the rapid transport of Li^+ through the electrode interface.

Keywords: Surface modification; $Li_{1.2}Mn_{0.54}Ni_{0.13}Co_{0.13}O_2$; Citric Acid; Electrochemical performance

1. INTRODUCTION

Lithium ion batteries have been widely used in a variety of portable electronic devices because of their high energy density, and are used in applications such as electric vehicles and as energy storage batteries [1-3]. The choice of electrode material is a key factor in the electrochemical performance of

batteries. The ternary cathode material $xLi_2MnO_3 \cdot (1-x)LiMO_2$ (M = Ni, Co, Mn, etc.), with its high specific capacity (which could theoretically reach 250 mAh/g), good rate capability, cycle performance, and low price, has attracted significant attention for power battery development [4-6]. However, this material suffers from low initial charge-discharge efficiency, and large irreversible capacity, which limit its more general application [7-8]. To solve these problems, scientists have investigated modifications such as elemental doping, surface coating, and surface oxygen vacancies, but the effect of these modifications has been less than satisfactory [9-21].

Pre-activation is an effective way to improve the initial efficiency and rate capability of lithium-rich cathode materials [22]. The initial efficiency of lithium rich cathode materials was improved using acid treatment [23-24]. However, the excessive acidity destroyed the surface morphology of the material and impaired the cycle stability and rate capability. The spinel-like substance $Li_4Mn_5O_{12}$ was generated on the surface of $Li[Li_{0.2}Ni_{0.2}Mn_{0.6}]O_2$ treated with HCl, H_2SO_4, and HNO_3, and the median voltage dropped noticeably [25]. The activation barrier for TM diffusion in the presence of oxygen vacancies reduced drastically [26]. A slight change in the structure of Na_2S-treated $Li_{1.2}Mn_{0.54}Ni_{0.13}Co_{0.13}O_2$ can help decrease the charge transfer resistance, thus enhancing the rate capability [27].

In the present work, $Li_{1.2}Mn_{0.54}Ni_{0.13}Co_{0.13}O_2$ was synthesized by using the carbonate co-precipitation method, and citric acid was used for pre-activation of this cathode material. The influence of citric acid pre-activation on the electrochemical properties of the cathode materials used in lithium batteries was investigated.

2. EXPERIMENTAL

2.1 Material Preparation

$MnSO_4 \cdot H_2O$, $NiSO_4 \cdot 6H_2O$, and $CoSO_4 \cdot 7H_2O$ were used as raw materials to fabricate the electrodes, with Na_2CO_3 as the precipitant and NH_4HCO_3 as the complexing agent. The pH of the solution was maintained at 8.0, and the temperature was held at 80 °C. The solution was stirred at 800 rpm to effect coprecipitation, after which the mixture was filtered, washed, and dried to obtain the $[Mn_{0.54}Ni_{0.13}Co_{0.13}](CO_3)_{0.8}$ precursor. The precursor was preheated with $LiOH \cdot H_2O$ of 3 wt.% excess at 500 °C for 5 h and sintered at 950 °C for 12 h to give the target product $Li_{1.2}Mn_{0.54}Ni_{0.13}Co_{0.13}O_2$.

2.0 g of anhydrous citric acid ($C_6H_8O_7$) was weighed out and dissolved in 100 mL deionized water. The pH of this solution was 1.97. Then, 5 g of the prepared $Li_{1.2}Mn_{0.54}Ni_{0.13}Co_{0.13}O_2$ cathode material was added, and the mixture was immersed in 80 °C water bath for 1 h, after which it was dried, ground until homogeneous, and sintered at 500 °C for another 5 h. The mixture was cooled, washed, and filtered with deionized water. The filtrate was collected for elemental analysis. The residue filtered out was vacuum-dried at 120 °C for 10 h to yield the processed material. The cathode materials treated with citric acid are denoted as "$C_6H_8O_7$-$Li_{1.2}Mn_{0.54}Ni_{0.13}Co_{0.13}O_2$."

2.2 Material characterization

Phase analysis of the product was performed with a Bruker D8 Advance XRD (Bruker Corporation, Germany). The Kα rays produced by the Cu target were used as the radiation source, at a scanning speed of $10°\cdot min^{-1}$. The step size was 0.02°, and the 2θ scanning range was 10°–80°. A JSM-7001F field emission scanning electron microscope (FE-SEM, JSM-7001F, JEOL, Japan) was used to inspect the size and microstructure of powdered material, with energy dispersive spectroscopy (EDS) to quantitatively analyze the elemental composition of the material. The element composition and element contents in the filtrate were examined by a multi-channel inductively coupled plasma atomic emission spectrometer (ICP-AES, Baird Corporation, Germany).

2.3 Electrochemical characterization

The electrochemical properties of $Li_{1.2}Mn_{0.54}Ni_{0.13}Co_{0.13}O_2$ material were tested using CR2025 button cells composed of the modified/unmodified $Li_{1.2}Mn_{0.54}Ni_{0.13}Co_{0.13}O_2$, lithium metal foil anode and Celgard 2320 membrane. The cathode was prepared as follows: a mixture of 75 wt.% $Li_{1.2}Mn_{0.54}Ni_{0.13}Co_{0.13}O_2$ material, 15 wt.% Super P conductive additive, and 10 wt.% polyvinylidene fluoride was stirred in 1-methyl-2-pyrrolidinone solvent with mixing to form the cathode slurry, which was then cast onto the aluminum foil and cut into 12-mm-diameter discs to form the cathode. The CR2025 cells were constructed in a glove box filled with argon gas, with $LiPF_6$ (1 M) in ethylene carbonate (EC)/dimethyl carbonate (DMC) (mass ratio 1:1) used as the electrolyte. The electrochemical properties were measured at 25 °C on a LAND CT-2001 battery testing system. Electrochemical impedance spectroscopy (frequency range: 0.01 Hz to 100 kHz; disturbance amplitude: 5 mV) and cyclic voltammetry (voltage range: 2-4.8 V; scanning rate: 0.1 mV/s) were performed on a CHI660D electrochemical workstation (Shanghai Chenhua, China).

3. RESULTS AND DISCUSSION

3.1 XRD structural characterization

The two XRD spectra shown in Fig. 1 for the product display clearly separated the (006)/(102) and (018)/(110) peaks, indicating the well-preserved layered structure of the material before and after citric acid modification [28-29]. The dominant phases exhibit a typical lamellar hexagonal α-$NaFeO_2$ structure belonging to the R-3m crystal system. The low-intensity peaks near 20° to 25° indicate a monoclinic crystal structure belonging to the C2/m space group [30-31], which arise from the well-ordered $LiMn_6$ cationic superlattice formed by the Mn^{2+} and the Li^+ infiltrated into the transition metal layers, as the $Li_{1.2}Mn_{0.54}Ni_{0.13}Co_{0.13}O_2$ cathode contains Li_2MnO_3 as one of its components. The intensity of this set of peaks reduces slightly after citric acid modification, which is because of the

lower amount of lithium present in the transition metal layer. Nevertheless, the structure of the material does not change much.

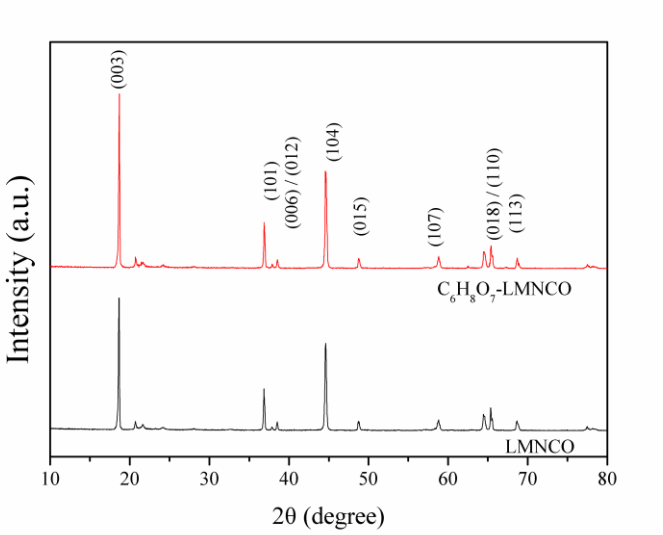

Figure 1. XRD patterns of $Li_{1.2}Mn_{0.54}Ni_{0.13}Co_{0.13}O_2$ samples before and after surface modification.

Table 1. Lattice parameters of $Li_{1.2}Mn_{0.54}Ni_{0.13}Co_{0.13}O_2$ before and after surface modification

Sample	a/Å	c/Å	c/a	$R=I_{(003)}/I_{(104)}$
$Li_{1.2}Mn_{0.54}Ni_{0.13}Co_{0.13}O_2$	2.853	14.220	4.984	1.520
$C_6H_8O_7$-$Li_{1.2}Mn_{0.54}Ni_{0.13}Co_{0.13}O_2$	2.849	14.243	4.999	1.679

From the lattice constants of the material before and after citric acid treatment and the $I_{(003)}/I_{(104)}$ ratios in Table 1, a decrease in the lattice constant a and an increase in c can be observed. This is because after the citric acid treatment, the diffusion and migration channels of Li^+ in the layered structure broaden, which improves the rate capability of the cathode material. Meanwhile, the c/a value is related to the stability of layered structure [32]. When the lattice constant c increases, both the diffraction intensity of the (003) peak and the value of $I_{(003)}/I_{(104)}$ ratio increase, which may be related to the migration of some protons (hydrogen ions) from $C_6H_8O_7$ into the laminar lattice, or the deintercalation of Li^+.

3.2 SEM images

As can be seen from the SEM image in Fig. 2, the cathode material formed by coprecipitation resembles spherical secondary particles with a size of about 0.5 μm. The surface morphology of the

modified $Li_{1.2}Mn_{0.54}Ni_{0.13}Co_{0.13}O_2$ changes little as compared with that of the unmodified $Li_{1.2}Mn_{0.54}Ni_{0.13}Co_{0.13}O_2$. The crystals are intact and exhibit a finer, uniform particle size.

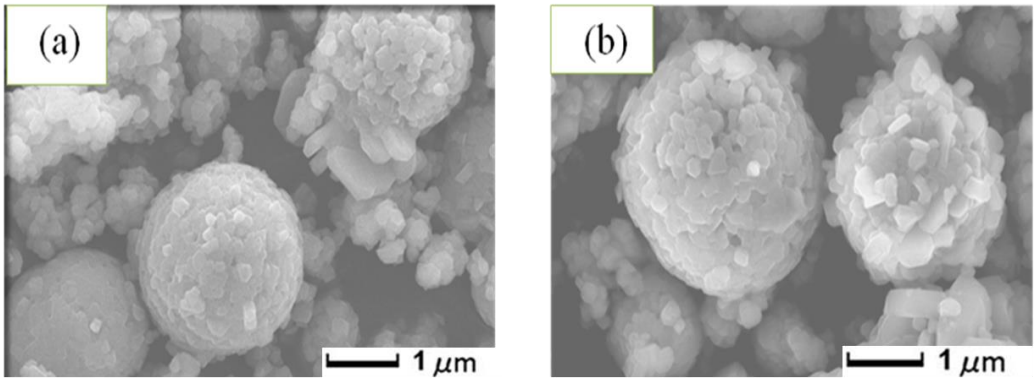

Figure 2. SEM images of $Li_{1.2}Mn_{0.54}Ni_{0.13}Co_{0.13}O_2$ before (a) and after surface modification (b).

3.3 ICP-MS analysis of filtrate composition

Elemental analysis was performed on the filtrate after modification. As shown in Table 2, the Li content reaches 13.37 wt.% in the filtrate after citric acid treatment. From the amount of material lost, the molecular formula of the processed material is established as $Li_{1.04}[Mn_{0.54}Ni_{0.13}Co_{0.13}]O_2$.

Table 2. Weight percent of elements dissolved out during surface modification process

Sample	Li/wt.%	Mn/wt.%	Ni/wt.%	Co/wt.%
$C_6H_8O_7$-$Li_{1.2}Mn_{0.54}Ni_{0.13}Co_{0.13}O_2$	13.37	0.0202	0.0224	0.0173

3.4 Initial charging-discharging performance

The charging plateaus of the material before and after citric acid modification exhibit two regions (Fig. 3). The first region is from 2.0 to 4.5 V, corresponding to the Li^+-extraction, along with the oxidation of Ni^{2+} to Ni^{4+} and Co^{3+} to Co^{4+} [33]. And the other region is at 4.5V, meaning the activation of the Li_2MnO_3 phase [34]. At 2.0-4.5 V, the curves display little change as no transition metal precipitates during citric acid treatment. At 4.5 V voltage, the charging plateau of the citric acid treated sample is significantly shortened, as 13.37 wt.% of Li is removed during the modification.

In the subsequent discharge process, Li_2O deintercalated from Li_2MnO_3 cannot be re-embedded into the cathode, resulting in a loss of charging capacity, and thus, an irreversible capacity loss of the material. As shown in Table 3, the initial irreversible capacity of the unmodified material is relatively large, at 117.0 mAh/g, and the coulombic efficiency is only 66.4%. This is because two Li ions are

activated with the Li_2MnO_3 phase at around 4.5 V and leak out during the first activation, but fewer octahedral vacancies are present during discharge for Li^+ re-intercalation.

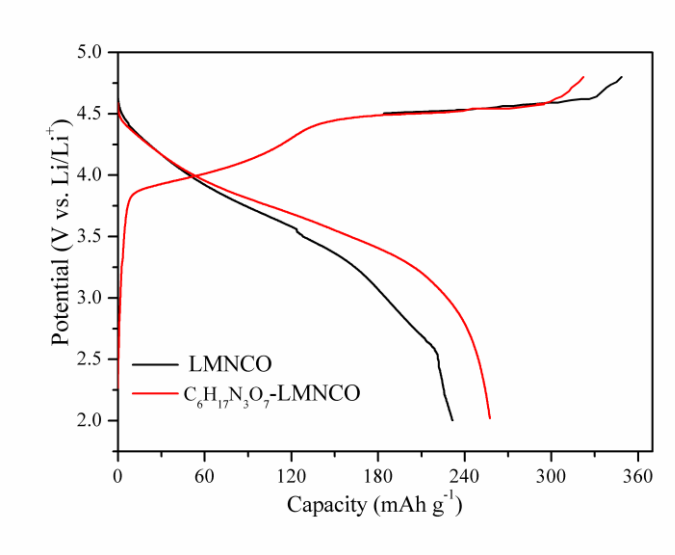

Figure 3. Initial charge and discharge profiles of $Li_{1.2}Mn_{0.54}Ni_{0.13}Co_{0.13}O_2$ samples before and after surface modification from 2.0 to 4.8 V at 0.1C rate.

Only one Li ion can be re-embedded into the layered structure, leading to low initial efficiency. After citric acid treatment, the initial efficiency increases to 79.9%, but the charging capacity is only 322 mAh/g. This could be due to the reaction of some Li^+ ions at the $Li_{1.2}Mn_{0.54}Ni_{0.13}Co_{0.13}O_2$ surface with citric acid to form a soluble substance, which is removed, causing a reduction in the total amount of de-intercalatable lithium during charging. The discharging capacity of the treated material is 257.4 mAh/g, as vacancies for Li^+ intercalation are generated by surface delithiation, which are capable of storing more lithium.

Table 3. Initial charge-discharge data of $Li_{1.2}Mn_{0.54}Ni_{0.13}Co_{0.13}O_2$ before and after surface modification

Sample	Specific charge capacity /mAh·g^{-1}	Specific discharge capacity /mAh·g^{-1}	Irreversible capacity /mAh·g^{-1}	Coulombic efficiency /mAh·g^{-1}	<4.5V /mAh·g^{-1}	4.5-4.8 V /mAh·g^{-1}
$Li_{1.2}Mn_{0.54}Ni_{0.13}Co_{0.13}O_2$	348.5	231.5	117.0	66.4	182.8	165.7
$C_6H_8O_7$-$Li_{1.2}Mn_{0.54}Ni_{0.13}Co_{0.13}O_2$	322.0	257.4	64.6	79.9	180.3	141.7

It can be seen from Table 3 that citric acid treatment does not affect the 2.0-4.5 V region significantly. The decrease in irreversible capacity loss is largely seen between 4.5 V and 4.8 V. This is

consistent with the removal of the Li_2O component from the Li_2MnO_3 phase of the material during citric acid treatment, which is precisely the key to the influence of the modification on the initial coulombic efficiency of the material.

3.5 Cycle performance of the material

Fig. 4 compares the cycle capacity before and after the treatment. As the number of cycles increases, the specific discharging capacity of the unmodified $Li_{1.2}Mn_{0.54}Ni_{0.13}Co_{0.13}O_2$ declines more rapidly and drops to 169.1 mAh/g after 100 cycles, equivalent to a capacity retention of only 84.85%. After treatment, the cycle performance of the material is enhanced. The specific discharging capacity is 202.6 mAh/g after 100 cycles, which corresponds to 90.81% capacity retention. Citric acid processing forms abundant manganese-rich, lithium-poor entities on the material surface, which boosts the structural stability of the interior and improves the material cycle performance.

As shown in Fig. 5, as the number of cycles increases, the discharge curves of the cathode material before and after the citric acid modification tend to shift toward lower voltage (as indicated by the arrows), implying greater cycle polarization. For the 1st and 100th cycles, the median voltage differences of the unmodified and modified materials are 0.27 V and 0.19 V, respectively, during discharging. Voltage attenuation in the material decreases after citric acid treatment, which is due to structural changes in the material in charging-discharging. Further, the median voltage of the material gradually decreases during cycling, which is consistent with the observations in previous studies [35].

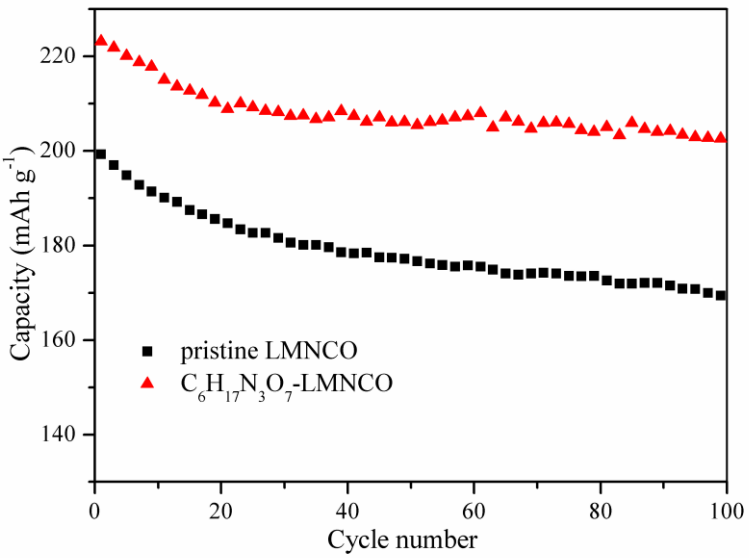

Figure 4. Cycle performance of $Li_{1.2}Mn_{0.54}Ni_{0.13}Co_{0.13}O_2$ samples before and after surface modification at 0.5C rate in the voltage range 2.0–4.6 V.

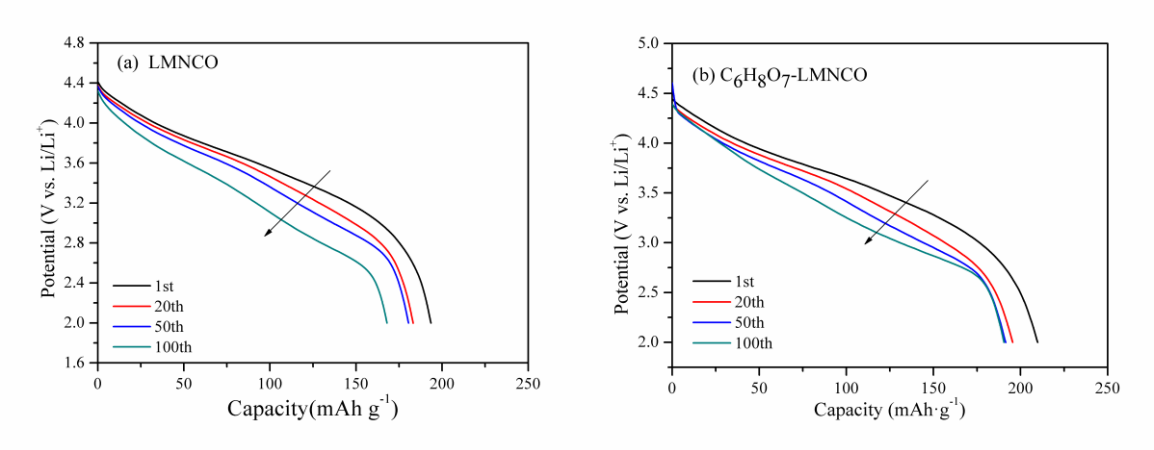

Figure 5. Discharge profiles of $Li_{1.2}Mn_{0.54}Ni_{0.13}Co_{0.13}O_2$ samples before (a) and after (b) surface modification in the 1st, 20th, 50th, and 100th cycles at 0.5C rate.

3.6 Rate capability of the material

The rate capabilities of the $Li_{1.2}Mn_{0.54}Ni_{0.13}Co_{0.13}O_2$ samples before and after surface modification are further investigated (Fig. 6). With increasing discharge current density, the discharge capacities of all the samples decreases due to polarization [36].

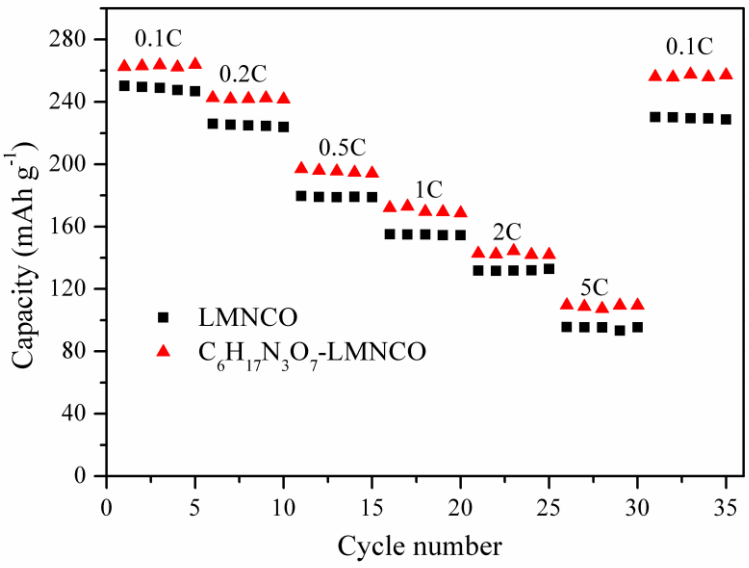

Figure 6. Rate capability of $Li_{1.2}Mn_{0.54}Ni_{0.13}Co_{0.13}O_2$ samples before and after surface modification at rates of 0.1, 0.2, 0.5, 1, 2, and 5 C in sequence every 5 cycles.

As can be seen from Figure 6, the rate capability of the citric acid-treated material is improved significantly. As shown in Table 4, when the current density increases to 5 C, the specific discharge capacity of the modified material is 108.9 mAh/g, which is higher than the 95.1 mAh/g of the unmodified one. As the current density increases, the charge transfer impedance in the cathode becomes higher and the specific discharging capacity declines rapidly. A chemical reaction takes place on the material surface after citric acid treatment, which results in the removal of some Li_2O, leaving behind the stable MnO_2 or $LiMn_2O_4$ spinel structures to act as Li^+ ion transport channels. This reduces the transfer impedance in the processed material and improves the rate capability. As reported previously [37-39], the spinel-like regions can decrease the charge transfer resistance and help improve the electrochemical performance of lithium-rich layered oxide materials.

Table 4. Discharge capacity of $Li_{1.2}Mn_{0.54}Ni_{0.13}Co_{0.13}O_2$ samples before and after surface modification at various current densities in the voltage range 2.0–4.6 V.

Discharge capacity/mAh·g^{-1}	0.1C rate	0.2C rate	0.5C rate	1C rate	2C rate	5C rate	Follow-up 0.1C rate
$Li_{1.2}Mn_{0.54}Ni_{0.13}Co_{0.13}O_2$	248.7	225.0	179.1	154.8	132.0	95.1	229.6
$C_6H_8O_7$-$Li_{1.2}Mn_{0.54}Ni_{0.13}Co_{0.13}O_2$	263.1	242.2	195.5	170.6	142.7	108.9	256.5

After charging and discharging cycles at different rates, the eventual specific discharging capacity of the processed material is 257.4 mAh/g at 0.1 C, corresponding to a capacity recovery of 97.49%. This that means the layered structure of the citric acid-modified material remains intact after cycling at a large current (5C rate) and retains a large capacity.

3.7 Electrochemical impedance of the material

The AC impedance change for the modified and unmodified materials was studied by electrochemical impedance spectroscopy (EIS), and the spectra are shown in Fig. 7. Fig. 8 shows the corresponding equivalent circuit diagram, based on which calculation and analysis were carried out. As shown in Fig. 7, the high-frequency semicircle, high-medium frequency semicircle, and low-frequency quasi-straight line on the Nyquist diagrams are the impedance for Li^+ ion diffusion at the electrode/electrolyte interface (R_{sf}, CPE_{sf}), charge transfer impedance (R_{ct}, CPE_{dl}), and Li^+ ion diffusion impedance within the material (W), respectively. Rs refers to the ohmic resistance of the cell, CPE_{sf} and CPE_{dl} are constant phase elements, and Zw is the semi-infinite Warburg diffusion impedance. Rs, Rsf, and Rct in this equivalent circuit were obtained by simulation with ZsimpWin software.

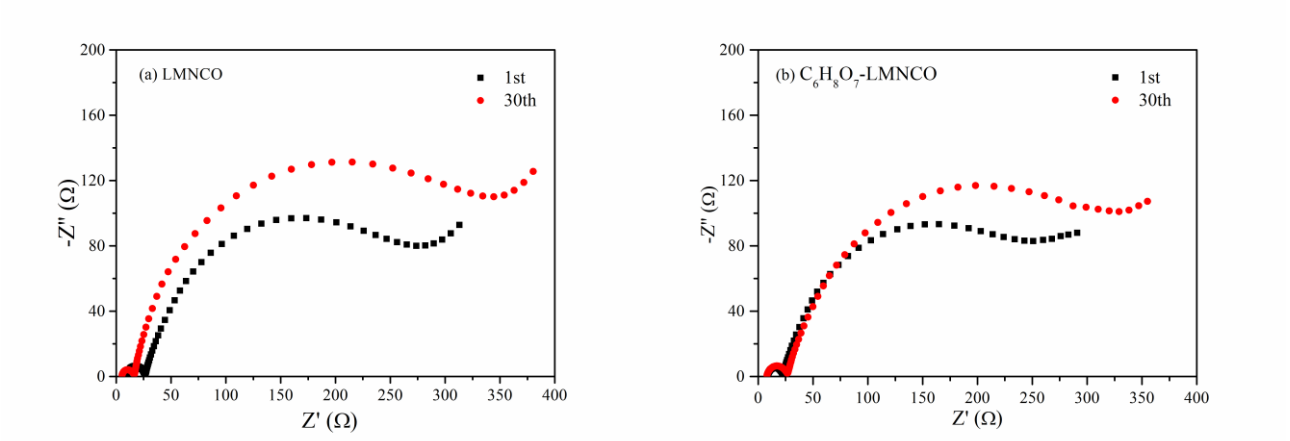

Figure 7. Nyquist plots of $Li_{1.2}Mn_{0.54}Ni_{0.13}Co_{0.13}O_2$ before and after surface modification at a charge state of 4.6 V in different cycles and the equivalent circuit.

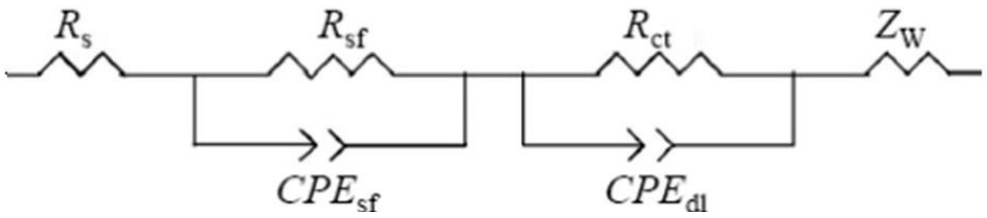

Figure 8. Equivalent circuit of $Li_{1.2}Mn_{0.54}Ni_{0.13}Co_{0.13}O_2$ samples before and after surface modification at a charge state of 4.6 V in different cycles.

With continued cycling, the $\triangle R_{sf}$ of the unmodified material becomes much larger than the modified. After 30 cycles, it can be seen that citric acid effectively lowers the impedance at the cathode and electrolyte interface. The $\triangle R_{sf}$ of the material drops to 65.4 Ω from the original 85.3 Ω. The weak acidity of this acid helps in cleaning the material surface and provides a stable channel for rapid Li^+ ion intercalation-deintercalation after its exchange reaction with hydrogen ions. This agrees with the increased capacity and rate capability after citric acid treatment.

During charging-discharging, both semi-infinite diffusion and limited diffusion take place in $Li_{1.2}Mn_{0.54}Ni_{0.13}Co_{0.13}O_2$. After citric acid treatment, both the interfacial charge transfer impedance (R_{ct}) and diffusion impedance (R_{sf}) are significantly reduced, indicating enhanced reaction kinetics in the material by citric acid modification. The smaller R_{ct} and R_{sf} values can be ascribed to the fact that the spinel-like regions of $Li_{1.2}Mn_{0.54}Ni_{0.13}Co_{0.13}O_2$ facilitate Li^+ ion transfer and diffusion through the interface [39-40].

4. CONCLUSIONS

In conclusion, citric acid pre-activation has been performed on the $Li_{1.2}Mn_{0.54}Ni_{0.13}Co_{0.13}O_2$ cathode material prepared by carbonate coprecipitation. Improvements in the electrochemical

performance of the cathode material, including the initial coulombic efficiency, rate capability, and cycle performance, are observed. The initial coulombic efficiency increases from 66.4% to 79.9%, and the capacity retention after 100 cycles at 0.5C increases from 84.85% to 90.81%. When the current density increases to 5C, the specific discharge capacity of the delithiated material is 108.9 $mAh \cdot g^{-1}$, which is much higher than that (95.10 $mAh \cdot g^{-1}$) before the treatment. This can be attributed to the opening up of more transport channels for Li^+ transport, smaller charge transfer impedance, higher Li^+ ion diffusion rate, and more stable material structure at the interface after the treatment of $Li_{1.2}Mn_{0.54}Ni_{0.13}Co_{0.13}O_2$ by citric acid.

References

1. J. Zheng, X. Wu and Y. Yang, *Electrochim. Acta*, 105 (2013) 200.
2. Y. Jiang, F. Zhou, C. Wang, J. Kong and L. Xu, *Ionics*, 23 (2017) 585.
3. Y. Zhou, P. Bai, H. Tang, J. Zhu and Z. Tang, *J. Electroanal. Chem.*, 782 (2016) 256.
4. V. Etacheri, R. Marom, R. Elazari, G. Salitra and D. Aurbach, *Energ. Environ. Sci.*, 9 (2011) 3243.
5. B. Liu, Z. Zhang, J. Wan and S. Liu, *Ionics*, 23 (2017) 1365.
6. J. Yang, F. Cheng, X. Zhang, H. Gao, Z. Tao and J. Chen, *J. Mater. Chem. A*, 6 (2014) 1636.
7. E. Han, Y. Li, L. Zhu and L. Zhao, *Solid State Ionics*, 255 (2014) 113
8. R. Yu, Y. Lin and Z. Huang, *Electrochim. Acta*, 173 (2015) 515.
9. J. Liu, J. Reeja and A. Manthiram, *J. Phys. Chem. C*., 114 (2010) 9528.
10. Y. Zhao, C. Zhao, H. Feng, Z. Sun and D. Xia, *Electrochem. Solid. St.*, 14 (2011) 1.
11. Y. Wu, A. Murugan and A. Manthiram, *J. Electrochem. Soc.*, 155 (2008) 635.
12. J. Zheng, J. Li, Z. Zhang, X. Guo and Y. Yang, *Solid State Ionics*, 179 (2008) 1794.
13. Y. Wu and A. Manthiram, *Electrochem. Solid. St.*, 9 (2006) 221.
14. Y. Jung, A. Cavanagh, Y. Yan, S. M. George and A. Manthiram, *J. Electrochem. Soc.*, 158 (2011) 1298.
15. Q. Wang, J. Liu, A. Murugan and A. Manthiram, *J. Mater Chem.*, 19 (2009) 4965.
16. W. Tang, L. Liu, S. Tian, L. Li, Y. Yue, Y. Wu, S. Guan and K. Zhu, *Electrochem. Commun.*, 12 (2010) 1524.
17. K. Du, X. Huang, F. Yang, G. Huang and Z. Peng, *Chinese J. Inorg. Chem*., 28 (2012) 983.
18. F. Zheng, X. Ou, Q. Pan, X. Xiong, C. Yang, Z. Fu and M. Liu, *Chem. Eng. J.*, 334 (2018) 497.
19. L. Ming, B. Zhang, Y. Cao, J. Zhang, C. Wang, X. Wang and H. Li, *Front. Microbiol.*, 6 (2018) 76.
20. Y. Wang, X. Huang, F. Li, J. Cao and S. Ye, *RSC. Adv.*, 5 (2015) 49651.
21. M. Sathiya, A. M. Abakumov, D. Foix, G. Rousse, K. Ramesha, M. Saubanère, M. L. Doublet, H. Vezin, C. P. Laisa, A. S. Prakash, D. Gonbeau, G. VanTendeloo and J. M. Tarascon, *Nat. Mater.*, 14 (2015) 230.
22. Z. Li, X. Li, Y. Liao, X. Li and W. Li, *J. Power Sources*, 334 (2016) 23.
23. Y. Wu, A. Murugan and A. Manthiram, *Electrochem. Soc.*, 155 (2008) 635.
24. S. Kang, C. Johnson, J. Vaughey, K. Amine and M. Thackeray, *J. Electrochem. Soc.*, 153 (2006) 1186.
25. G. Hu, W. Wang, K. Du, Z. Peng and Y. Cao, *Scientia. Sinica.*, 44 (2014) 1362.
26. D. Qian, B. Xu, M. Chic and Y. Meng, *Phys. Chem. Chem. Phys.*, 16 (2014) 14665.
27. Y. Li, S. Li, B. Zhong and Y. Chen, *J. Solid. State. Electr.*, 22 (2018) 547.

28. Y. Gao, M. Yakovleva and W. Ebner, *Electrochem. Solid-State Lett.*, 3 (1998) 117.
29. C. Lu and H. Wang. *J. Electrochem. Soc.*, 152 (2005) 341.
30. S. Kang, H. Qin, Y. Fang, X. Li and Y. Wang, *Electrochim. Acta*, 144 (2014) 22.
31. X. Jin, Q. Xu, X. Liu, X. Yuan and H. Liu, *Ionics*, 22 (2016) 1369.
32. X. Jin, Q. Xu, H. Liu, X. Yuan and Y. Xia, *Electrochim. Acta*, 136 (2014) 19
33. L. Cong, X. Gao, S. Ma, X. Guo, Y. Zeng, L. Tai, R. Wang, H. Xie and L. Sun, *Electrochim. Acta*, 115 (2014) 399.
34. N. Yabuuchi, K. Yoshii, S. Myung, I. Nakai and S. Komaba, *J. Am. Chem. Soc.*, *133* (2011) 4404.
35. M. Thackeray, S. Kang, C. Johnson, J. Vaughey, R. Benedek and S. Hackney, *J. Mater. Chem.*, 17 (2007) 3112.
36. X. Liu, H. Li, D. Li, M. Ishida and H. Zhou, *J. Power Sources*, 243 (2013) 374.
37. J. Zheng, S. Deng, Z. Shi, H. Xu, H. Xu, Y. Deng, Z. Zhang and G. Chen, *J. Power Sources, 221* (2013). 108
38. D. Yu, K. Yanagida, H. Nakamura and S. Fujitanni, *J. Electrochem. Soc.*, 157 (2010) 1177.
39. Y. Li, S. Li, B. Zhong, X. Guo, Z. Wu, W. Xiang, H. Liu and G. Liu, *J. Solid State Electrochem.*, 22 (2018) 547.
40. J. Liu, B. Reeja-Jayan and A. Manthiram, *J. Phys. Chem. C*, 114 (2010) 9528.